

Floquet Engineering of Quantum Materials

Takashi Oka^{1,2} and Sota Kitamura¹

¹¹ *Max-Planck-Institut für Physik komplexer Systeme, Nöthnitzer Straße 38, 01187 Dresden, Germany*

²² *Max-Planck-Institut für Chemische Physik fester Stoffe, Nöthnitzer Straße 40, 01187 Dresden, Germany*

Floquet engineering, the control of quantum systems using periodic driving, is an old concept in condensed matter physics, dating back to ideas such as the inverse Faraday effect. There is a renewed interest in this concept owing to the rapid developments in laser and ultrafast spectroscopy techniques and discovery and understanding of various “quantum materials” hosting interesting exotic quantum properties. Here, starting from a nontechnical introduction with emphasis on the Floquet picture and effective Hamiltonians, we review the recent applications of Floquet engineering in ultrafast, nonlinear phenomena in the solid state. In particular, Floquet topological states, application to ultrafast spintronics, and to strongly correlated electron systems are overviewed.

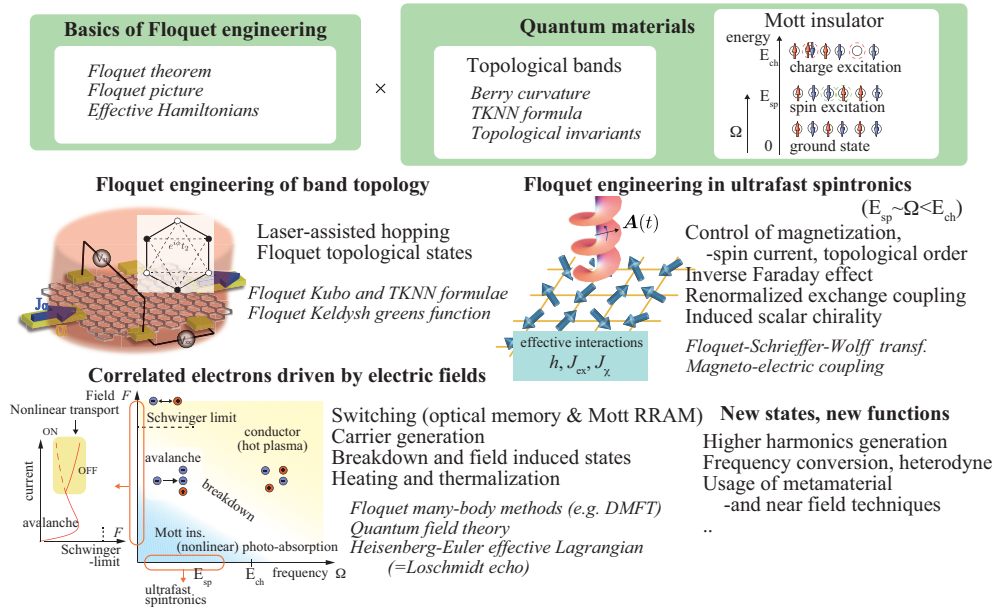


FIG. 1. Floquet engineering in quantum materials: Various processes take place when an intense laser or electric field is applied to quantum materials with exotic properties such as topological bands [17, 18], Dirac and Weyl semimetals [19–21] and strong correlation [22]. The italic keywords denote theoretical tools useful to describe them.

I. INTRODUCTION

How fast and drastic can we change electronic properties of materials, and what would be the most efficient way to do this? This is an interesting fundamental question and at the same time has connections to the electronic technology that supports our everyday life. Semiconductor devices surrounding us such as solar cells, transistors, and memories typically involve non-equilibrium processes triggered through light-matter coupling, and the application of electromagnetic fields changes their properties (transport, carrier density, magnetization, etc.) drastically. There is a growing interest in ultrafast [1–13] and non-linear [14–16] electronics, aiming to find a way to control post-semiconductor materials hosting exotic quantum properties.

Although this research area has a long history, recently there has been some theoretical developments enabling us to understand various phenomena systematically. One powerful tool is the concept of *Floquet engineering*, i.e., the control of quantum systems using time-periodic external fields. Theoretically, continuous irradiation of a laser can be modeled by a time periodic perturbation and the Hamiltonian $H(t)$ describing the irradiated system inherits the time periodicity

$$H(t + T) = H(t), \quad (1)$$

where the periodicity $T = 2\pi/\Omega$ is related to the photon energy or driving frequency Ω (we set $\hbar = 1$). During the past decades, with the help of the Floquet theorem [23–26], which is a temporal analogue of the Bloch theorem, the understanding of periodically driven systems has advanced considerably especially for open transport problems [27, 28], laser driven atoms [29], strongly correlated electron systems [9, 30–38], electron-phonon systems [37, 39–41] and their universal mathematical structures for closed systems [42–49]. It is possible to dynamically induce interesting exotic quantum states by carefully selecting the driving laser that matches the target material. While Floquet engineering is now applied in several fields of physics, most notably in cold atoms in optical traps [50, 51], here we focus on its application in electronic systems that is illustrated in **Figure 1**.

II. BASICS OF FLOQUET ENGINEERING

We consider systems periodically driven by external fields with a Hamiltonian satisfying the periodicity condition Equation 1. The basic idea of the Floquet method is to expand quantities into Fourier modes $e^{-im\Omega t}$ with $m = 0, \pm 1, \dots$. The Floquet picture (or Shirley picture) is not only useful in doing systematic calculations, but also gives an intuitive way of understanding driven systems [23]. In one-body problems, it gives a *mapping to a quantum model*

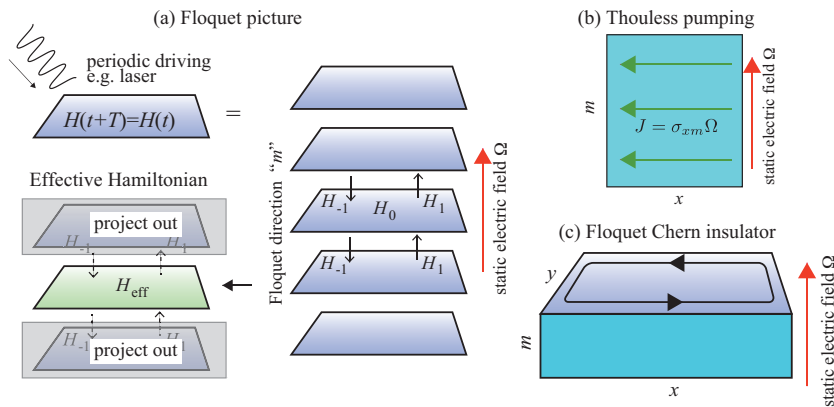


FIG. 2. Floquet picture for one body physics: A mapping (a) to a static higher dimensional model gives an intuitive understanding of (b) Thouless pumping (Section II A) and (c) Floquet Chern insulators (Section III). The effective Hamiltonian describes physics projected on to the original Hilbert space (Section II D).

with one extra dimension. The index m of the Fourier mode can be considered as a lattice site index in a fictitious “Floquet direction” (**Figure 2**). Let us see this in more details.

When the Hamiltonian is time periodic, as in the Bloch theorem, one can take the set of solutions of the time dependent Schrödinger equation to be a product of a time periodic function and a non-periodic phase factor, i.e.,

$$|\Psi(t)\rangle = e^{-i\varepsilon t}|\Phi(t)\rangle, \quad |\Phi(t+T)\rangle = |\Phi(t)\rangle. \quad (2)$$

The time periodic function $|\Phi(t)\rangle$ is called the Floquet state and ε the Floquet quasi-energy. Note that ε has an indefiniteness of integer multiples of Ω . We use the Fourier expansion

$$H(t) = \sum_m e^{-im\Omega t} H_m, \quad |\Phi(t)\rangle = \sum_m e^{-im\Omega t} |\Phi^m\rangle \quad (3)$$

for the Hamiltonian and the Floquet state. With this representation, the time dependent Schrödinger equation is mapped to an eigenvalue problem [23, 25]

$$\sum_m (H_{n-m} - m\Omega\delta_{mn}) |\Phi_\alpha^m\rangle = \varepsilon_\alpha |\Phi_\alpha^n\rangle \quad (4)$$

in an extended Hilbert space. The index α labels eigenstates and m, n are the Fourier mode indices. Now, the Hilbert space has been infinitely expanded, but this is compensated by the indefiniteness of ε .

One can view the index m as a position in the Floquet direction: The system described by Equation 4 is equivalent to a time independent layered one body system where m labels the layers (**Figure 2**). The intra layer hopping is described by H_0 , while H_m ($m \neq 0$) give inter layer couplings. In addition, there is a static electric field in the Floquet direction coming from the $m\Omega$ -term in Equation 4. This fictitious electric field Ω plays an important role in understanding the physics of driven systems. For small Ω , we have a lattice problem in higher dimensions in a weak electric field. If this model is a two dimensional Chern insulator with a Hall coefficient σ_{xm} , a dissipationless current $j_x = \sigma_{xm}\Omega$ is generated, which is nothing but the Thouless pumping [52]. For larger Ω , the layers become isolated energetically and the state exhibits the Wannier-Stark localization (along the Floquet direction). In such a situation, the high-frequency expansion is a powerful tool in understanding the physics systematically.

A. Thouless pumping in the Floquet picture

The Thouless pumping [52] is probably one of the most well known phenomenon in time-periodic systems. The Rice-Mele model [53] defined by

$$H(t) = - \sum_j (J + \delta_1 \cos \Omega t (-1)^j) (c_{j+1}^\dagger c_j + \text{h.c.}) + \delta_2 \sin \Omega t \sum_j (-1)^j c_j^\dagger c_j \quad (5)$$

is a minimum model that shows charge pumping (J : static hopping, $\delta_{1,2}$: modulation parameter of the hopping and on-site potential). By interpreting Ωt as momentum in the Floquet direction, this model can be mapped to a two

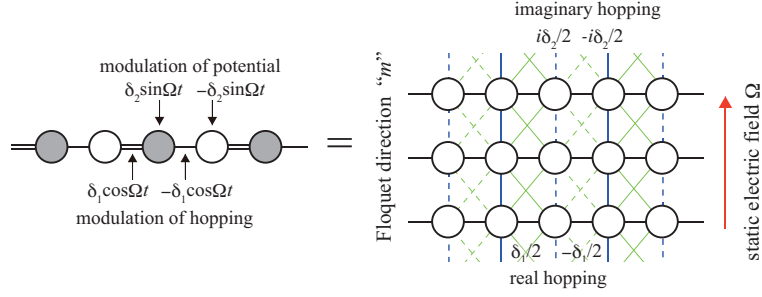


FIG. 3. Floquet picture for Thouless pumping in the Rice-Mele model.

dimensional lattice system (**Figure 3**) governed by the eigenvalue problem Equation 4, with $H_0 = -J \sum_j (c_{j+1}^\dagger c_j + \text{h.c.})$, $H_{\pm 1} = (1/2) \sum_j (-1)^j [-\delta_1 (c_{j+1}^\dagger c_j + \text{h.c.}) \pm i \delta_2 c_j^\dagger c_j]$. With this description, the Thouless pumping is nothing but the two dimensional quantum Hall effect in the m - x plane [54]. The Hall conductivity of this effective m - x plane is given by

$$\sigma_{xm} = i \sum_{\lambda} f_{\lambda} \int_0^T dt \int \frac{dk}{2\pi} \left[\left\langle \frac{\partial \psi_{\lambda}}{\partial t} \middle| \frac{\partial \psi_{\lambda}}{\partial k} \right\rangle - \left\langle \frac{\partial \psi_{\lambda}}{\partial k} \middle| \frac{\partial \psi_{\lambda}}{\partial t} \right\rangle \right], \quad (6)$$

which is nothing but the original expression derived by Thouless [52] and is equivalent to the TKNN (Thouless-Kohmoto-Nightingale-den Nijs) formula [55] with the y coordinate replaced by m . It becomes quantized ($\sigma_{xm} = \frac{2\pi}{h} m$, $m = 0, \pm 1, \pm 2, \dots$) as long as the gap do not close and the distribution f_{λ} is a constant within the band, *i.e.* the field strength Ω is smaller than the Landau-Zener tunneling threshold. In such situation, the relation $J = \sigma_{xm} \Omega$ states that integer number of charge is transferred per unit time $T = 2\pi/\Omega$.

B. High-frequency expansion

Let us consider a situation where the driving frequency Ω is much larger than other typical energy scales in the Hamiltonian, so that the layers are isolated energetically. In this situation the eigenvalue problem of Equation 4 can be solved efficiently by performing (van Vleck's) degenerate perturbation theory starting from the unperturbed Hamiltonian with only the $m\Omega$ -term [56, 57]. After performing the perturbative expansion, the eigenvalue problem becomes *decoupled* in the Floquet direction. This means that the quasi-energy can be obtained as eigenvalues of the static Hamiltonian. This effective Hamiltonian has a universal form for time-periodic Hamiltonians (including many-body systems),

$$H_{\text{eff}}^{\text{vV}} = H_0 + \sum_{m \neq 0} \left(\frac{[H_{-m}, H_m]}{2m\Omega} + \frac{[[H_{-m}, H_0], H_m]}{2m^2\Omega^2} + \sum_{n \neq 0, m} \frac{[[H_{-m}, H_{m-n}], H_n]}{3mn\Omega^2} \right) + \mathcal{O}(\Omega^{-3}). \quad (7)$$

For later convenience, we provide the effective Hamiltonian for free fermions described by $H(t) = \sum_{ij} J_{ij}(t) c_i^\dagger c_j$ with $J_{ij}(t+T) = J_{ij}(t) = \sum_m J_{ij}^m e^{-im\Omega t}$. The effective Hamiltonian is calculated to be [35]

$$H_{\text{eff}}^{\text{vV}} = \sum_{ij} \left(J_{ij}^{(0)} + J_{ij}^{(1)} + J_{ij}^{(2)} \right) c_i^\dagger c_j + \mathcal{O}(\Omega^{-3}), \quad (8)$$

where the effective hopping is given as

$$J_{ij}^{(0)} = J_{ij}^0, \quad J_{ij}^{(1)} = \sum_{m \neq 0} \sum_k \frac{J_{ik}^{-m} J_{kj}^m}{m\Omega},$$

$$J_{ij}^{(2)} = \sum_{m \neq 0} \sum_{kl} \left(\sum_{n \neq 0} \frac{J_{ik}^{-m} J_{kl}^{m-n} J_{lj}^n}{mn\Omega^2} - \frac{J_{ik}^0 J_{kl}^{-m} J_{lj}^m + J_{ik}^{-m} J_{kl}^m J_{lj}^0}{2m^2\Omega^2} \right). \quad (9)$$

C. Application to many-body systems

When we consider many-body systems driven periodically, we must be careful since the system may heat up. In closed periodically driven systems, a state will evolve as $|\psi(t)\rangle = \sum_{\alpha} c_{\alpha} e^{-i\varepsilon_{\alpha}t} |\Phi_{\alpha}(t)\rangle$, where $c_{\alpha} = \langle \Phi_{\alpha}(t_0) | \psi_0 \rangle$ and $|\psi_0\rangle$ is the initial state at time $t_0 = 0$. $|\Phi_{\alpha}(t)\rangle$ are the Floquet states with quasi-energy ε_{α} . On stroboscopic time steps ($t = mT$), the solution $|\psi(t)\rangle$ has an identical form as the time evolution in static systems with the quasi-energy ε_{α} playing the role of the (usual) energy and $|\Phi_{\alpha}(t_0)\rangle$ usual eigenstate.

In static nonintegrable many-body systems, for typical initial states, **thermalization** is expected to occur after a sufficiently-long time evolution [58, 59]. This implies that the periodically-driven systems are also expected to thermalize because $\langle \psi(t) | \hat{O} | \psi(t) \rangle |_{t \rightarrow \infty} = \sum_{\alpha} e^{-\beta \varepsilon_{\alpha}} \langle \Phi_{\alpha}(t_0) | \hat{O} | \Phi_{\alpha}(t_0) \rangle$ should hold for an observable \hat{O} in the stroboscopic time evolution. However, remember that ε_{α} was only defined modulo Ω , and such indefiniteness should not appear in physical quantities. The solution to this paradox was given in References [42, 43] showing that $\langle \Phi_{\alpha}(t_0) | \hat{O} | \Phi_{\alpha}(t_0) \rangle$ is independent of α . In other words, all many-body Floquet states that we obtain by solving Equation 4 are featureless. This can be stated more intuitively that in closed systems, periodically driven many-body states will thermalize to an infinite temperature state, which is consistent with a natural consequence in thermodynamics.

Nevertheless, Floquet theory is still a useful framework in many-body systems. **Heating** should occur in a very long time scale in an appropriately chosen driving, so that there can be a nontrivial metastable state in the shorter time scale. By using an appropriate perturbative expansion and truncating out the slow heating processes coming from higher order terms, we can describe this metastable state as an eigenstate of the effective Hamiltonian [45–47]. In this situation, a periodically driven system will first “equilibrate” with the truncated Hamiltonian, and eventually thermalize to the true long time limit, i.e., the infinite temperature state. The first equilibration is termed as the **Floquet prethermalization**, as a special case of **prethermalization** [60] known in quench dynamics [61, 62] [reviewed in [63, 64]].

Electrons in solid states are subject to various **open system** relaxation processes such as phonon scattering or coupling to an electron bath (substrate). When the pump is longer than their characteristic coupling time, the system converges to a nonequilibrium steady state, and the heating will be balanced with the relaxation [39, 40]. The nontrivial steady states of such systems can be studied by the Floquet Greens function method combined with an appropriate many-body technique such as non-equilibrium dynamical mean field theory [9, 30]. In Section V, we try to sort out results in ultrafast and nonlinear experiments in correlated electron systems from the point of view of many-body Floquet dynamics.

D. Effective Hamiltonians

While we have already introduced the concept of the effective Hamiltonian in Section IIB, here we discuss its general aspect in more details. We have obtained the form of the effective static Hamiltonian (Equation 7) by the block-diagonalization of Equation 4 with regarding the inter-layer transitions as virtual processes. If we consider this in the time domain, the construction of the effective Hamiltonian can be recasted to a search for an appropriate time-periodic unitary transformation

$$\tilde{H} = U^{\dagger}(t)H(t)U(t) - iU^{\dagger}(t)\frac{\partial}{\partial t}U(t) \quad (10)$$

that makes \tilde{H} time-independent. While the existence of the transformation is assured by the Floquet theorem, such a transformation is not unique. One arbitrariness comes from the time-independent unitary transformation, by which we can generate new effective Hamiltonians once we obtain one static Hamiltonian. There is also an arbitrariness due to the indefiniteness of the quasi-energy.

One conventional effective Hamiltonian is the Floquet-Magnus (FM) Hamiltonian [65, 66], which can be obtained from the time-evolution operator over a period T as

$$H_{\text{eff}}^{\text{FM}} = \frac{i}{T} \ln \hat{T} \exp \left[-i \int_{t_0}^{t_0+T} H(s) ds \right], \quad (11)$$

where \hat{T} denotes time ordering. While the form of the Hamiltonian changes depending on the initial time t_0 , those with different t_0 are related by unitary transformations. The van Vleck Hamiltonian (Equation 7) is also unitary-equivalent to the FM Hamiltonian up to the truncation error.

The effective Hamiltonian depends on the perturbation schemes; An approximation more efficient than the high frequency expansion can be constructed if we use the eigenbasis of $H_0 - m\Omega$, the intra-layer term¹ in the Floquet picture (**Figure 2**), as the starting point of perturbation. Note that the high-frequency expansion (Equation 7) is using $m\Omega$ as the unperturbed Hamiltonian. For example, if a perturbation to H_0 is given by $V(t) = ve^{i\Omega t} + v^\dagger e^{-i\Omega t}$, the second-order contribution yields

$$\langle a | \delta H_{\text{eff}}^{2\text{nd}} | b \rangle = - \sum_c \left[\frac{\langle a | v | c \rangle \langle c | v^\dagger | b \rangle}{\Delta_{cb} - \Omega} + \frac{\langle a | v^\dagger | c \rangle \langle c | v | b \rangle}{\Delta_{cb} + \Omega} \right] \quad (12)$$

where $H_0 | a \rangle = E_a | a \rangle$, $\Delta_{ab} = E_a - E_b$. This form is employed, e.g., in the theory of inverse Faraday effect [67]. Application of this expansion 12 requires all the eigenstates of H_0 , which are often difficult to obtain. We can still use a solvable part within the Hamiltonian to construct the basis and perform an expansion around it. For example, the Floquet-Schrieffer-Wolff transformation (strong coupling expansion) for the Hubbard model [68–71] expands in series of $1/(n_D U - m\Omega)$ (n_D doublon number), and the atomic Hamiltonian $U \sum_i n_{i\uparrow} n_{i\downarrow} - m\Omega$ is used to define the basis (to be explained in Section IV).

Among a variety of the effective Hamiltonians, we should adopt an appropriate one in accordance with a problem of interest. The FM Hamiltonian is directly related to the time evolution, and suitable for the initial-value problem and quench dynamics. Since the FM Hamiltonian often does not respect the symmetry of the system, it is better to use the van Vleck expansion when we are interested in the properties of the Hamiltonian itself.

III. FLOQUET ENGINEERING OF BAND TOPOLOGY

In this section, as a representative example of Floquet engineering, we discuss properties of the graphene irradiated by a circularly polarized laser [72]. In particular, we focus on transport and response properties, and introduce theoretical tools to relate the nontrivial Floquet states and response functions.

A. Laser irradiated graphene

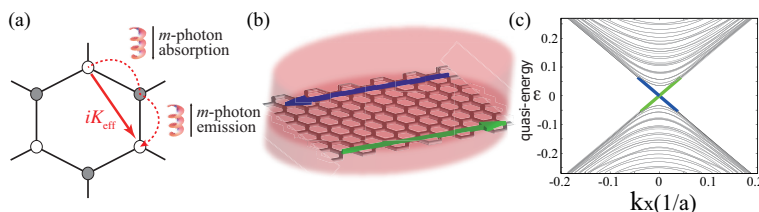


FIG. 4. (a) Laser-assisted hopping (dotted lines) for the honeycomb lattice driven by a circularly polarized laser leads to an effective next nearest hopping with a phase factor (Equation 14). Haldane’s Chern insulator model [73] is obtained up to first order in the high frequency expansion. (b) Chiral edge modes are induced under irradiation and this is seen in the (c) Floquet quasi-energy spectrum [74].

In graphene [19] carbon atoms form a honeycomb lattice whose low-energy effective model is described by a tight-binding model of the p_z orbital $H = - \sum_{ij}^{\text{NN}} J_{ij} c_i^\dagger c_j$. Here, we take the sum over nearest-neighbor (NN) sites and $J_{ij} = J$ is the hopping amplitude. The energy dispersion of this model has two inequivalent Dirac cones in the Brillouin zone, at K and K’ [$\mathbf{k} = (\pm 4\pi/3\sqrt{3}, 0)$]. The honeycomb tight-binding model in circularly polarized laser is a prototype of the Floquet topological insulator [72, 74–76]. Let us see this by first employing the high-frequency expansion (Section II B). We introduce the laser electric field $\mathbf{E}(t) = -\partial_t \mathbf{A}(t)$ using the Peierls substitution as

$$J_{ij}(t) = J_{ij} \exp \left(-i \int_{\mathbf{R}_j}^{\mathbf{R}_i} \mathbf{A}(t) \cdot d\mathbf{r} \right), \quad (13)$$

¹ There are also more general choices with non-block-diagonal Hamiltonians (not decoupled in the Floquet direction), which are treated in a same way after a block diagonalization of the unperturbed Hamiltonian.

where \mathbf{R}_i is the position of site i , and the vector potential representing a circularly polarized laser is given as $\mathbf{A}(t) = (A \cos \Omega t, A \sin \Omega t)$. Then the Fourier components of the hopping amplitude is given as $J_{ij}^n = J \mathcal{J}_n(A) e^{im\phi_{ij}}$ with the bond angle $\phi_{ij} = -\tan^{-1}(R_i^x - R_j^x)/(R_i^y - R_j^y)$ and \mathcal{J}_m being the m -th Bessel function of the first kind. The Fourier expansion of the hopping represents laser-assisted processes, absorbing or emitting m -photons. We can then use Equation 9 to obtain an effective Hamiltonian as

$$H_{\text{eff}} = - \sum_{ij}^{\text{NN}} J_{\text{eff}} c_i^\dagger c_j + \sum_{ij}^{\text{NNN}} iK_{\text{eff}} \tau_{ij} c_i^\dagger c_j + J\mathcal{O} \left(\frac{J^2}{\Omega^2} \right), \quad (14)$$

where τ_{ij} in the next-nearest-neighbor (NNN) term takes $+1$ (-1) for the hopping with a clockwise (counterclockwise) path (from j to i) on each hexagons. The effective hopping amplitudes are

$$J_{\text{eff}} = J \mathcal{J}_0(A), \quad iK_{\text{eff}} = -i \frac{2J^2}{\Omega} \sum_{n=1}^{\infty} \frac{\mathcal{J}_n^2(A)}{n} \sin \frac{2\pi n}{3}. \quad (15)$$

J_{eff} is obtained as a time average of the original Hamiltonian, where a renormalization factor $\mathcal{J}_0(A)$ appears as is known as the dynamic localization [24, 30] (possibly has been observed in solids [77]). The effective NNN hopping iK_{eff} emerges from the two-step laser-assisted hopping process **Figure 4(a)**. Equation 15 is nothing but the Hamiltonian of the Haldane model [73], and at the Dirac cones K and K' the model exhibits a topological gap opening leading to a nontrivial Chern number. Chiral edge modes emerges in the quasi-energy spectrum **Figure 4(b),(c)**, and their direction as well as the sign of the Chern number depends on the sign of K_{eff} that can be flipped by changing the polarization $\Omega \rightarrow -\Omega$.

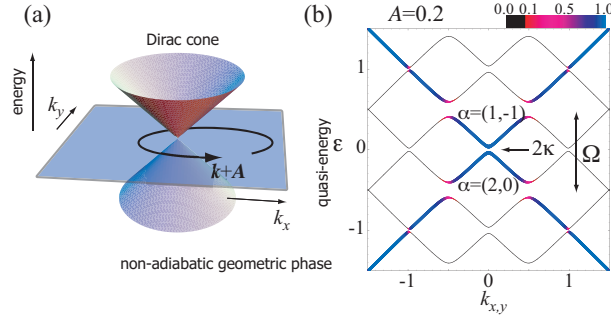


FIG. 5. (a) States with momentum \mathbf{k} acquires a geometric phase near the Dirac node. (b) Floquet spectrum of two dimensional Dirac system in circularly polarized laser. Color coding represents the static weight (adapted from Reference [72]).

While the high-frequency expansion gives an intuitive picture for the Floquet topological phase transition, let us comment on the role played by the geometric phase on the gap opening. In momentum space, Through the Peierls substitution (Equation 13), a state with momentum \mathbf{k} start to move as $\mathbf{k} + \mathbf{A}(t)$ in the momentum space. For the circularly polarized laser, this motion is circular (**Figure 5(a)**), and the state acquires the Aharonov-Anandan phase [78] (or the non-adiabatic extension of the Berry phase [79]) during the time evolution. The Floquet quasi-energy is written as

$$\varepsilon_\alpha = \langle \langle \Phi_\alpha | H(t) | \Phi_\alpha \rangle \rangle + \Omega \gamma_\alpha^{\text{AA}} / 2\pi, \quad (16)$$

a sum of the dynamical phase and the Aharonov-Anandan phase. We have used the time averaged inner product and matrix element of a time dependent operator as $\langle \langle \Phi_\alpha | \Phi_\beta \rangle \rangle \equiv \frac{1}{T} \int_0^T dt \langle \Phi_\alpha(t) | \Phi_\beta(t) \rangle = \sum_m \langle \Phi_\alpha^m | \Phi_\beta^m \rangle$, and $\langle \langle \Phi_\alpha | \mathcal{O} | \Phi_\beta \rangle \rangle = \frac{1}{T} \int_0^T dt \langle \Phi_\alpha(t) | \mathcal{O}(t) | \Phi_\beta(t) \rangle$, respectively. At the Dirac points K and K' [$\mathbf{k} = (\pm 4\pi/3\sqrt{3}, 0)$] (with a linearized dispersion), the Aharonov-Anandan phase becomes [72]

$$\gamma_\alpha^{\text{AA}} \equiv T \langle \langle \Phi_\alpha | i\partial_t | \Phi_\alpha \rangle \rangle = \pm\pi \left\{ [4(A/\Omega)^2 + 1]^{-1/2} - 1 \right\}. \quad (17)$$

In the adiabatic limit ($\Omega \rightarrow 0$), it converges to the Berry phase $\mp\pi$. The size of the gap 2κ can be evaluated as

$$2\kappa = \sqrt{4A^2 + \Omega^2} - \Omega. \quad (18)$$

In solid states, the gap opening of Dirac node as well as the other replica bands shown in **Figure 5(b)** was observed in a time resolved ARPES experiment [80]. In artificial matters, the periodically driven graphene was simulated in cold atoms in optical lattices [81] as well as in photonic wave guides [82], realizing the Haldane model (Floquet Chern insulator).

B. Floquet Kubo and TKNN formulae

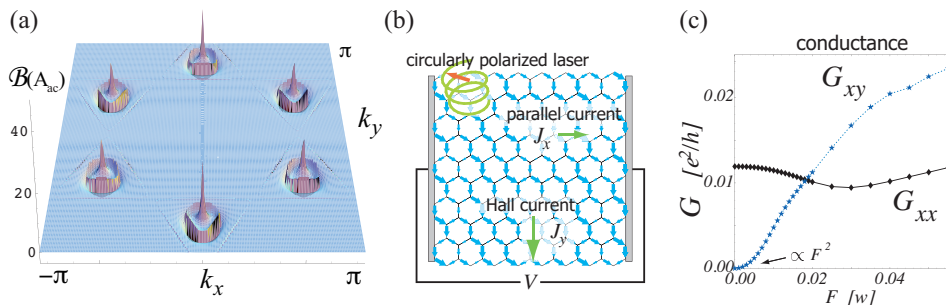


FIG. 6. (a) Berry curvature of the Floquet band in graphene irradiated by circularly polarized laser (adapted from Reference [72]). Detection of Floquet Chern insulator can be done with (b) transport measurements of the (c) Hall conductance G_{xy} [72]. ($F = \Omega A_{ac}$).

In equilibrium, the quantum Hall effect at zero temperature is related to the Chern number through the TKNN formula. In a similar way, we need the Floquet-Kubo formula [83] and the Floquet TKNN formula [72] to characterize the response of Floquet topological states. Here, we discuss nonlinear optical and transport properties in the presence of irradiation. When a *strong* laser is applied (A_{ac}) to a system, its response to an additional *weak* perturbation can be changed. The response function is defined by a linear relation

$$j_i(\omega) = \sigma_{ij}(A_{ac}; \omega) E_j(\omega) \quad (19)$$

between the weak probe electric field E_j and the induced current j_i . The effect of the external AC-field is taken into account using Floquet states as the basis. The optical response function for irradiated systems in the DC-limit ($\omega \rightarrow 0$) becomes

$$\sigma_{ij}(A_{ac}) = i \int \frac{d\mathbf{k}}{(2\pi)^d} \sum_{\alpha \in BZ_1} \sum_{\beta \neq \alpha} \frac{f_\beta(\mathbf{k}) - f_\alpha(\mathbf{k})}{\varepsilon_\beta(\mathbf{k}) - \varepsilon_\alpha(\mathbf{k})} \frac{\langle\langle \Phi_\alpha(\mathbf{k}) | J_j | \Phi_\beta(\mathbf{k}) \rangle\rangle \langle\langle \Phi_\beta(\mathbf{k}) | J_i | \Phi_\alpha(\mathbf{k}) \rangle\rangle}{\varepsilon_\beta(\mathbf{k}) - \varepsilon_\alpha(\mathbf{k}) + i0^+}, \quad (20)$$

which was given in References [72, 74, 84]. Here, ε_α is the quasi-energy of Floquet states α , and f_α is its occupation fraction. Note that the index α is limited to the first Brillouin zone ($\varepsilon_\alpha \in [-\Omega/2, \Omega/2]$) whereas β is taken over the whole Floquet spectrum which is extended from the original spectrum by the inclusion of photon-dressed replica states. The Hall coefficient is given by the Floquet-TKNN formula [72]

$$\sigma_{xy}(A_{ac}) = e^2 \int \frac{d\mathbf{k}}{(2\pi)^2} \sum_{\alpha \in BZ_1} f_\alpha(\mathbf{k}) [\nabla_{\mathbf{k}} \times \mathcal{A}_\alpha(\mathbf{k})]_z. \quad (21)$$

The artificial gauge field and its associated Berry curvature is defined by

$$\mathcal{A}_\alpha(A_{ac}; \mathbf{k}) = -i \langle\langle \Phi_\alpha(\mathbf{k}) | \nabla_{\mathbf{k}} | \Phi_\alpha(\mathbf{k}) \rangle\rangle, \quad \mathcal{B}_\alpha(A_{ac}; \mathbf{k}) = \nabla_{\mathbf{k}} \times \mathcal{A}_\alpha(\mathbf{k}). \quad (22)$$

Figure 6(a) shows the Berry curvature of a Floquet band, where we can see that peaks appear at the Dirac points. There are also concentric patterns around the Dirac points where resonant hybridization occurs between the bands. There are two promising detection schemes of the Hall effect, which is the transport measurement in the presence of irradiation (**Figure 6(b,c)** illustrates), and the time resolved Kerr effect [84, 85]. In the Kerr effect, the polarization angle shifts as [86]

$$\Theta_H \sim (\sigma_{xy} \text{ in units of } \frac{e^2}{h}) \times 6.3 \text{ mrad} \quad (23)$$

in the presence of a quantum Hall state. The Hall conductivity is not necessarily quantized in a Floquet Chern insulator since the electrons are photo-excited and the distribution function f_α is not the simple zero-temperature Fermi distribution. However, there has been several numerical analysis finding conditions for a quantized Hall coefficient in open systems [84, 87].

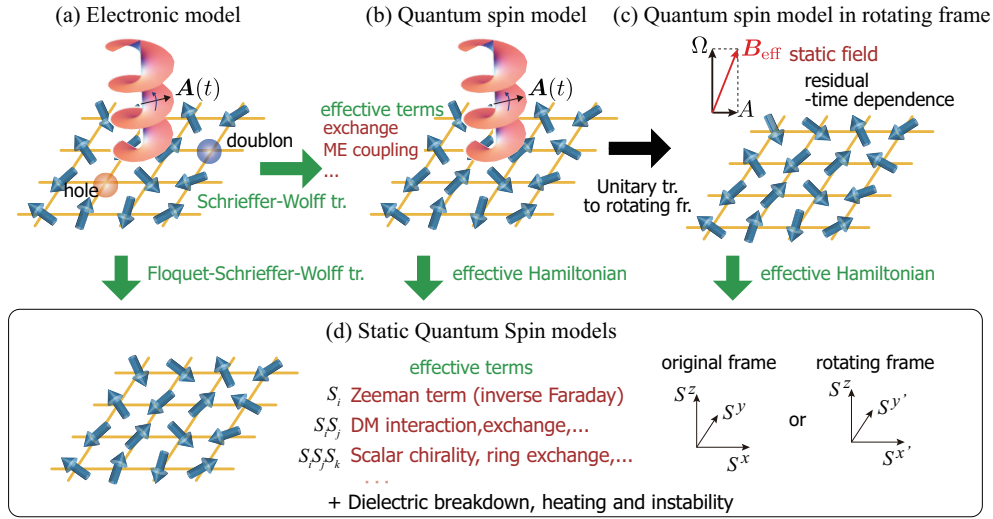


FIG. 7. Effective theories for Floquet engineering in ultrafast spintronics: (a) The starting system is the electronic models, e.g., band ferromagnets and Mott insulators, under irradiation. (b) Time dependent spin model is obtained by assuming that the field is weak and Ω much smaller than the charge gap. (c) For circularly polarized laser, moving to the rotating frame gives a static magnetic field. (d) Effective Hamiltonians can be obtained by using appropriate expansion schemes.

IV. FLOQUET ENGINEERING IN ULTRAFAST SPINTRONICS

Spintronics is a new branch of electronics where the spin degrees of freedom is used to carry and store information via spin current and magnetization [88]. In ultrafast spintronics, laser is used to control spins and magnetism in the time scale of pico-seconds or faster [6, 89, 90]. A direct way to access spins is by the Zeeman coupling that couples to the magnetic field component of laser. Another relevant coupling is the magneto-electric (ME) coupling which arrows the electric field to interact with the polarization that depends on the spins. Several types of ME couplings are proposed [reviewed in [91]] such as (i) inverse Dzyaloshinskii-Moriya (DM) model [92, 93] $\mathbf{P} \propto \mathbf{e}_{\mathbf{r},\mathbf{r}'} \times (\mathbf{S}_{\mathbf{r}} \times \mathbf{S}_{\mathbf{r}'})$ and (ii) exchange striction model $\mathbf{P} \propto \boldsymbol{\pi}_{\mathbf{r},\mathbf{r}'} \times (\mathbf{S}_{\mathbf{r}} \cdot \mathbf{S}_{\mathbf{r}'})$.

The idea of Floquet engineering and effective Hamiltonians can be applied to ultrafast spintronics. Since the spin degrees of freedom originates from electrons, the construction of the effective Hamiltonian has different levels of approximation illustrated in **Figure 7**.

(a) Electronic model: If direct electronic excitations are involved, we should start the construction from the electronic model. A classic example is the inverse Faraday effect studied by Pershan *et al.* [67], where they used Equation 12 to obtain an effective Zeeman coupling $\delta H_{\text{eff}} = h_{\text{eff}} S_z$ for electron systems in circularly polarized laser applied along the z -axis. The effective magnetic field h_{eff} , obtained by considering virtual electronic excitations, is a nonlinear function of the laser strength and frequency and can be extremely large [6, 89, 90]. On the other hand, in strongly correlated insulators such as the Mott insulator, using the second order perturbation Equation 12 is difficult, and thus it is plausible to combine the Floquet picture with the standard Schrieffer-Wolff transformation [68–71], which will be explained in Section IV A.

(b) Quantum spin model: Another way to construct the effective theory is to start from quantum spin models including the coupling to laser fields [94, 95], i.e.,

$$H(t) = H_0 - g\mu_B \mathbf{B}(t) \cdot \mathbf{S} - \mathbf{E}(t) \cdot \mathbf{P}. \quad (24)$$

Here, H_0 denotes the original quantum spin models, e.g., Heisenberg model, and the other terms are the Zeeman and ME coupling. This approach is justified when the field is much slower than the electron dynamics ($\Omega \ll E_{\text{ch}}$). An effective Hamiltonian for circularly polarized laser based on the high frequency expansion (Equation 7)

$$\delta \mathcal{H}_{\text{eff}} = -\frac{i}{2\Omega} \{ \beta^2 [S^x, S^y] + \alpha\beta ([\tilde{P}^x, S^x] + [\tilde{P}^y, S^y]) + \alpha^2 [\tilde{P}^x, \tilde{P}^y] \} \quad (25)$$

$$\sim 1 \text{ spin term} + 2 \text{ spin term} + 3 \text{ spin term} \quad (26)$$

can be obtained [95]. Here, the dimensionless polarization is defined by $\tilde{\mathbf{P}} = \mathbf{P}/g_{\text{me}}$ with g_{me} being the ME coupling constant and $\alpha = g_{\text{me}} E_0$ and $\beta = g\mu_B E_0 c^{-1}$. Evaluating the commutators, we obtain terms that are product of 1, 2,

3 spins, for example the Zeeman, DM and spin chirality, and their precise forms depend on the ME coupling reflecting the symmetry of the crystal.

(c) Quantum spin model in the rotating frame: In the special case where the applied field is circularly polarized, we can obtain an exact form of the effective Hamiltonian without carrying out the perturbative expansion: A quantum spin system in rotating magnetic field described by $H(t) = H_0 + A \cos(\Omega t) S_x + A \sin(\Omega t) S_y$ can be mapped to a simple static magnetization problem $\tilde{H} = H_0 + \Omega S_z + A S_x$ by moving to the rotating frame using a unitary transformation $U(t) = \exp(i\Omega S_z t)$ assuming that H_0 is rotationally symmetric around the z -axis. The effective magnetic field $h_{\text{eff}} = (A, 0, \Omega)$ acting on the mapped system can be large, e.g., Ω in terahertz corresponds to few teslas, and can be used to orient the spins and induce magnetization[96, 97].

A. Floquet-Schrieffer-Wolff transformation

Here, we will see how the laser electric field influences the spin degree of freedom via the framework of the strong-coupling expansion for the periodically-driven Hubbard model. We introduce the Hubbard model under a laser electric field,

$$H(t) = T(t) + UD = - \sum_{ij\sigma} t_{ij} e^{-iA_{ij}(t)} c_{i\sigma}^\dagger c_{j\sigma} + U \sum_i n_{i\uparrow} n_{i\downarrow}, \quad (27)$$

where t_{ij} describes hopping of electrons c from site j to i , while U the on-site density interaction. The oscillating electric field is described by the Peierls phase $A_{ij}(t)$.

First, let us quickly review the strong-coupling expansion of the Hubbard model in the static case. In the strong coupling limit of the Hubbard model $t_{ij} = 0$, the ground states are any electron configurations with no double occupancy, which have a macroscopic degeneracy. In particular, the subspace spanned by the ground states at half filling is described by spin configurations. The macroscopic degeneracy lifts when we introduce the hopping $t_{ij} \neq 0$ as a perturbation. The low-energy effective model that describes this lift is the Heisenberg model, where the antiferromagnetic exchange interaction J_{ij} is given as $J_{ij} = 4t_{ij}^2/U$.

To perform a perturbative expansion of macroscopically degenerate systems in a systematic manner, it is convenient to employ the canonical transformation (Schrieffer-Wolff transformation). Namely, we consider a unitary transformation e^{iS} as a series in t_{ij} , and determine it order by order to block-diagonalize the Hamiltonian with respect to double-occupancy D , which classifies the eigenstates in the atomic limit. We then obtain the effective spin Hamiltonian as the $D = 0$ sector of the transformed Hamiltonian. Our goal in this section is to see the influence of an external field on the Mott insulator described by this strong-coupling expansion.

One can extend this scheme to a time-dependent situation by considering a time-dependent transformation. We first perform a series expansion of the transformed Hamiltonian $H'(t)$ in $S(t)$ as [98, 99]

$$\begin{aligned} H'(t) &= e^{iS(t)} H(t) e^{-iS(t)} - e^{iS(t)} i \partial_t e^{-iS(t)} \\ &= H(t) + [iS(t), H(t) - i\partial_t] + \frac{1}{2} [iS(t), [iS(t), H(t) - i\partial_t]] + \dots, \end{aligned} \quad (28)$$

and further expand $S(t)$ in t_{ij} as $S(t) = S^{(1)}(t) + S^{(2)}(t) + \dots$. Then the first-order term of $H'(t)$ is given as

$$H^{(1)} = T(t) + [iS^{(1)}(t), UD] - \partial_t S^{(1)}(t). \quad (29)$$

To block-diagonalize $H'(t)$, we determine S by solving a set of differential equations

$$\partial_t S_{+d}^{(1)}(t) = -idUS_{+d}^{(1)}(t) + T_{+d}(t) \quad (30)$$

for $d \neq 0$, where S_{+d} , T_{+d} denote terms which increase double occupancy D by d . While one can solve these for arbitrary fields with an appropriate boundary condition, here we consider a monochromatic laser $A_{ij}(t) = A_{ij} \cos(\Omega t - \phi_{ij})$ in particular, and consider a time-periodic solution. By carrying out the second-order perturbation, we obtain the Heisenberg model with a modified exchange interaction [68]

$$J_{ij}(t) = \sum_{m,n} (-1)^m \frac{4|t_{ij}|^2 \mathcal{J}_{n+m}(A_{ij}) \mathcal{J}_{n-m}(A_{ij})}{U - (m+n)\Omega} \cos 2m(\Omega t - \phi_{ij}), \quad (31)$$

where \mathcal{J}_m is m th Bessel function. This is the lowest-order contribution of the electric field on the spin interaction. The obtained spin interaction is time periodic, and the effective static Hamiltonian can be obtained by performing the high-frequency expansion (Section II B).

While we have considered a simple spin interaction in the Hubbard model here, there are various mechanism to produce effective spin interactions via virtual processes, such as the Kugel-Khomskii coupling in the multi-band systems [100, 101], superexchange coupling in multiferroic systems [93], and anisotropic spin coupling under the strong spin-orbit coupling [102, 103], for all of which we can apply the described scheme.

As we have mentioned in Section II C, the heating processes in higher order perturbation are (implicitly) truncated out in the present scheme. Such processes associated with charge excitations emerge as a divergence of the expansion (due to a vanishing energy denominator $DU - m\Omega$). This divergence originally comes from an additional degeneracy between sectors with different D in the atomic limit². Hence, we have to be aware that, in the true degenerate perturbation theory, one cannot block-diagonalize the Hamiltonian with D (nor m), and the above scheme is valid up to a certain finite order [70]. The inter-sector (changing D) terms is nothing but the charge excitations, which leads to the heating. It is a general property of the effective Hamiltonian approach that the heating processes emerge as a divergence of the series expansion, and the error due to the truncation of the expansion gives a finite (but very long in many cases) lifetime [45–47, 51].

1. Control and detection of spin chirality using laser

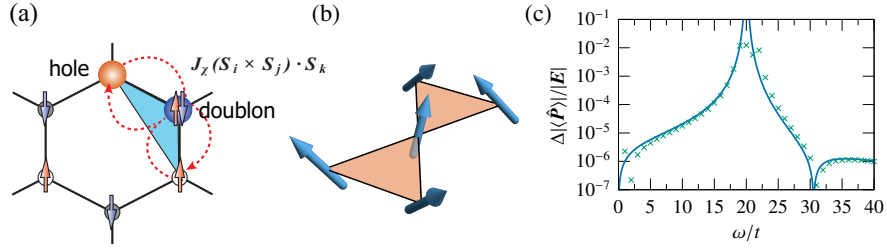


FIG. 8. (a) Laser assisted virtual hopping process leading to the scalar spin chirality term. (b) classical configuration of spins with nonzero scalar chirality, $(\hat{\mathbf{S}}_i \times \hat{\mathbf{S}}_j) \cdot \hat{\mathbf{S}}_k$. (c) Circular dichroism: Difference of the induced electric polarization between left and right circularly-polarized lasers, as a function of the photon energy. Crosses are numerical results for a three-site Hubbard cluster, and the solid curve is obtained from Equation 34.

While we have confirmed the modification of the exchange interaction, more intriguing possibility is to induce an emergent interaction term that is absent in the static model by irradiating a laser. This can be achieved by applying a field which breaks some symmetry of the original system. For instance, the time-reversal symmetry is broken when the circularly-polarized laser is applied. If we continue the strong-coupling expansion to the fourth-order **Figure 8(a)**, the emergent term is the scalar spin chirality term $\chi_{ijk} = \mathbf{S}_i \cdot (\mathbf{S}_j \times \mathbf{S}_k)$. A classical spin configuration with a nonzero scalar chirality is shown in **Figure 8(b)** for illustration. Upon irradiation, a effective scalar chirality term $\delta H_{\text{eff}} = \sum_{ijk} J_{\chi,ijk} \chi_{ijk}$ with

$$J_{\chi,ijk} = -4|t_{ij}|^2|t_{jk}|^2 \sum_{l,n} \sum_{m \neq 0} \left[\frac{\mathcal{J}_{l+m}(A_{ij})\mathcal{J}_l(A_{ij})\mathcal{J}_{n+m}(A_{jk})\mathcal{J}_n(A_{jk}) \sin m(\phi_{ij} - \phi_{jk})}{(U - l\Omega)(U - n\Omega)(U - (l+n+m)\Omega)} + \frac{\mathcal{J}_{l+m}(A_{ij})\mathcal{J}_{l-m}(A_{ij})\mathcal{J}_{n+m}(A_{jk})\mathcal{J}_{n-m}(A_{jk}) \sin 2m(\phi_{ij} - \phi_{jk})}{m\Omega(U - (l+m)\Omega)(U - (n+m)\Omega)} \right] \quad (32)$$

emerges[70, 71]. This opens an intriguing possibility of Floquet engineering exotic quantum phases such as a chiral spin liquid phase³ [105].

The light-induced interaction has a potential application as a new probe: For the above example, the circularly-polarized laser acts as a conjugate field to the scalar spin chirality for general Mott insulators, as in the magnetic field conjugate to the spin. Namely, the coupling constant for the scalar chirality is reduced to be

$$J_{\chi,ijk} \sim \frac{2\mathcal{A}_{ijk}|t_{ij}|^2|t_{jk}|^2\Omega(7U^2 - 3\Omega^2)}{U^2(U^2 - \Omega^2)^3} i(\mathbf{E}^* \times \mathbf{E})_z, \quad (33)$$

² For example, when $U/\Omega = p/q$ with coprime p, q , the quasienergy $\epsilon = DU - m\Omega$ is zero not only for $(D, m) = (0, 0)$ but also for $(q, p), (2q, 2p), \dots$

³ Floquet chiral spin liquid with Majorana edge modes is proposed in Kitaev systems [104] under circularly polarized laser [94]. This theory starts from the driven quantum spin model.

in the leading order of the field amplitude, where \mathcal{A}_{ijk} is the area enclosed by sites i, j, k . The interaction term describes the modulation of the dielectric function proportional to the scalar chirality, when it is seen as a term in the Hamiltonian of the electromagnetic field. From Equation 33, the modulation is obtained as an imaginary off diagonal part leading to the circular dichroism [70]

$$\epsilon_{xy}(\omega) = i \sum_{ijk} \frac{4|t_{ij}|^2|t_{jk}|^2\omega(7U^2 - 3\omega^2)}{U^2(U^2 - \omega^2)^3} \mathcal{A}_{ijk} \langle (\hat{\mathbf{S}}_i \times \hat{\mathbf{S}}_j) \cdot \hat{\mathbf{S}}_k \rangle. \quad (34)$$

Namely, one can read out the presence of the scalar chirality via the circular dichroism. **Figure 8(c)** shows the difference of the dielectric function between circularly polarized light with a different chirality.

Validity of the expansion and candidate materials: The effective Hamiltonian approach is only valid in a time scale shorter than that of heating. In Mott insulators, creation of doublon-hole pairs will make the system conducting and destroy the spin picture. There are several sweet spots suitable for Floquet engineering in ultrafast spintronics. (i) High frequency regime: When Ω exceeds both U and t , several doublon-hole pairs must be created simultaneously, which is a slower process. Heating becomes exponentially slow in this case [63]. Candidate materials are organic Mott insulators [106] since their energy scale is one order smaller compared to cuprates. (ii) Sub-gap regime $\Omega < \Delta_{\text{Mott}}$: This is an attractive regime since many Mott insulators have gaps around and above 1 eV [22], and one can use mid-infrared lasers to access the spins.

When the field becomes stronger, charge excitation becomes nonnegligible due to higher order processes such as multi-photon absorption, tunneling, and even electron avalanche. This is critical for spintronics application, but opens a new possibility for a “photo-induced phase transition”, which we explain in the next section.

V. CORRELATED ELECTRONS DRIVEN BY ELECTRIC FIELDS

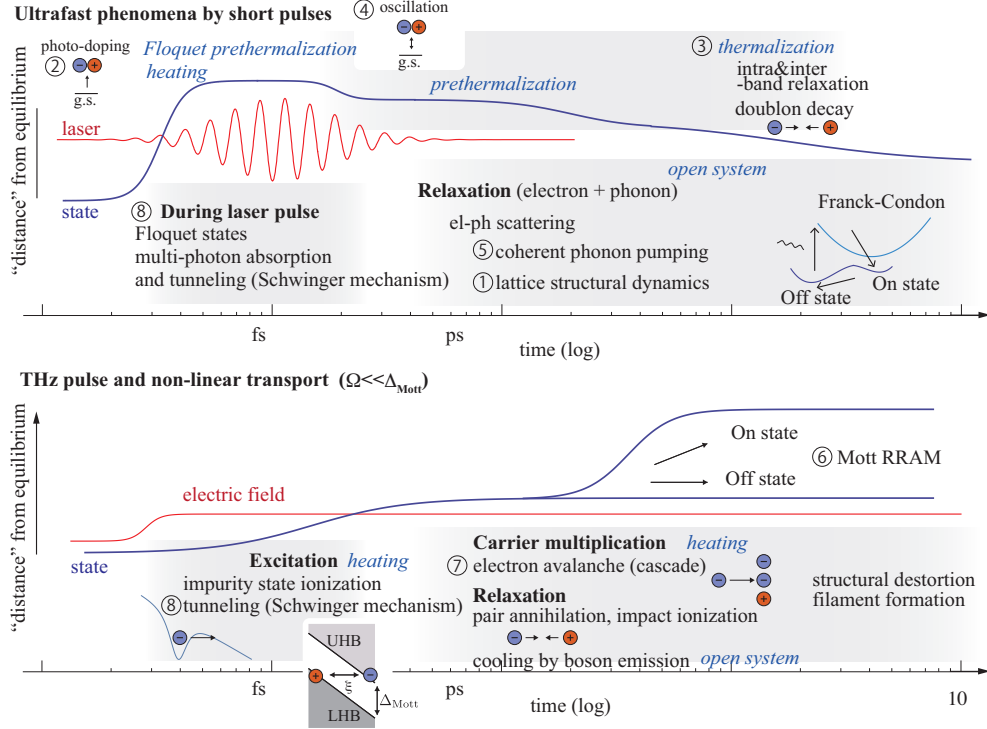


FIG. 9. Processes taking place in pump-probe experiments with ultra-short pulses and with longer pulses or non-linear DC devices (lower panel). The blue italic keywords roughly correspond to the many-body processes explained in Section II C.

Ultrafast phenomena in strongly correlated electron systems driven by intense laser pulses have been studied during the last decades starting from a pioneering work in organic molecular compounds [107, 108] and vanadium oxides [109] that are associated with ① structural lattice dynamics. In many cases, the structural change can be explained

through the Franck-Condon picture [1]; When electrons are excited, the lattice is subject to the Hellmann–Feynman force different from equilibrium and is moved from the original structure (OFF) to a metastable excited state (ON). This switching can be used to realize an “optical memory”. In cuprates the concept of ② “photo-doping”, i.e., creating doublon (electron)-hole pairs as transient carriers by laser, was introduced [110]. Since then, the time resolution, intensity and the flexibility to adjust the photon energy Ω of the pump laser have improved drastically [reviewed in [1–5, 7, 9–13]].

Let us explain the sequential processes that take place during and after the pulse laser with the corresponding numbers shown in **Figure 9** with the general Floquet many-body physics explained in Section II C in mind. First, we note that the physics strongly depends on the pulse duration, ranging from few femto seconds in the near infrared regime ($\Omega \sim 1.5\text{eV}$) to pico seconds (10^3 fs) for THz lasers ($1\text{THz} = 4.1\text{meV}$). The typical timescale of electron dynamics is femto seconds, and thus for electrons irradiated by THz lasers the duration of the pulse is long enough that we expect to see the DC-field physics realized in transistor-like devices with applied bias voltage [14–16].

Using ultrashort pulses (**Figure 9** upper), it is now possible to observe quantum coherent dynamics in strongly correlated electron systems such as ③ ultrafast switching and relaxation towards a Mott insulator [111] or toward a metal [112] and it is even possible to see the ④ interference oscillation between the Mott insulating groundstate and the excited state with a doublon-hole pair [113]. Interestingly, almost at the same time, relaxation dynamics and doublon decay in a strongly interacting fermionic system was observed in cold atoms in optical traps, and this was realized by dynamically changing the trap [114]. The dynamical control of lattice structure is also used in solid states, and this is done by exciting ⑤ coherent phonon oscillations to optimize the lattice structure with an aim to drive the electronics into interesting nonequilibrium phases such as a superconductor [13, 115–117].

In the DC limit (**Figure 9** lower) accessible by THz pump or non-linear transport devices, the electrons will be excited continuously and at the same time experience various relaxation processes, and their balance may realize interesting nonequilibrium steady states. The main relaxation mechanism is through emission of bosons, *e.g.* phonon, photon and spin fluctuation. In DC devices made from strongly correlated materials, one goal is to realize a ⑥ Mott RRAM (resistivity random access memory); A device with an IV -characteristics showing switching behaviors [14–16, 118–120]. This can be considered as a DC limit of the optical switch. The electron avalanche ⑦ is an important excitation mechanism that makes the carrier density to exponentially increase leading to switching to a conducting state [121] (also demonstrated in a THz laser-excited semiconductor [122]).

It is still not easy to experimentally study the ⑧ electron dynamics during the pulse duration in strongly correlated materials since the typical pulse duration is few to tens of femtoseconds. On the other hand, theoretical studies using the driven Hubbard model (Equation 27) have been done extensively [31, 123–128].

(a) Laser driven conducting state at resonance ($\Omega \sim \Delta_{\text{Mott}}$): In the presence of an AC electric field resonant with the Mott gap, the system evolves to a photo-induced metallic state within a short time scale. The doublon and hole pairs are resonantly created by the field, and at the same time, will be destroyed through stimulated emission, and the system reaches a transient metastable state [31]. In 1D, this state shares common feature as the equilibrium Tomonaga-Luttinger liquid such as spin charge separation. Such a metallic state can be captured by combining the Floquet method with the fermion-boson correspondence [31] or using the Floquet-Schrieffer-Wolff transformation [129].

(b) Dielectric breakdown and Keldysh crossover ($\Omega < \Delta_{\text{Mott}}$) [123, 124, 128]: Starting from the Mott insulating groundstate, the application of sub-gap AC electric fields will trigger dielectric breakdown through quantum tunneling or multi-photon absorption. The Loschmidt echo captures how a state $|\psi(t)\rangle = e^{-iHt}|\psi(0)\rangle$ is excited from the initial state, and is defined by their overlap $\langle\psi(0)|e^{-iHt}|\psi(0)\rangle$. If the overlap decays as $\langle\psi(0)|e^{-iHt}|\psi(0)\rangle \sim e^{-i\mathcal{L}'t - \mathcal{L}''t}$ ($\mathcal{L}', \mathcal{L}''$: real), then $\Gamma = 2\mathcal{L}''$ characterizes the decay of the initial state, while \mathcal{L}' is the Aharonov-Anandan phase [78]. In quantum electrodynamics (QED) in an external field background, the Loschmidt echo was studied, and defines the Heisenberg-Euler-Schwinger effective Lagrangian [130–133]. This was adapted to (interacting) lattice models using the groundstate-to-groundstate amplitude [5, 124]

$$\mathcal{L}(F) = - \lim_{\tau \rightarrow \infty} \frac{i}{\tau V} \ln \langle 0 | \hat{T} e^{-i \int_0^\tau F(s) \hat{X}(s) ds} | 0 \rangle, \quad (35)$$

where $F = A\Omega$ is the electric field, V the volume and $\hat{X} = \sum_i i n_i$ is the position operator in the interaction representation $\hat{X}(t) = e^{itH_0} \hat{X} e^{-itH_0}$, where the original lattice Hamiltonian H_0 , *e.g.* Hubbard Hamiltonian, is used. The real part of the effective Lagrangian is related to the field induced electron polarization $P(F) = \frac{\partial}{\partial F} \text{Re} \mathcal{L}(F)$ and reduces to the Berry phase formula [134, 135] in the weak DC field limit. The imaginary part of the effective Lagrangian gives the decay rate $\Gamma(F)/V = 2\text{Im} \mathcal{L}(F)$ of the insulating ground state. The leading contribution to $\Gamma(F)/V$ comes from the doublon-hole creation, a process known in QED as the Schwinger effect [132, 133]. For the 1D Hubbard model, one can use Bethe ansatz of the non-Hermitian Hubbard model combined with the imaginary

time method to evaluate the creation probability of doublon-hole pairs [126, 128]

$$\mathcal{P}_{\text{dh}} \sim \begin{cases} \left(\frac{F_0 \xi}{\hbar \Omega}\right)^{2 \frac{\Delta_{\text{Mott}}}{\Omega}} & \gamma \gg 1 (\text{multiphoton}), \\ \exp\left(-\frac{\pi}{2} \frac{\Delta_{\text{Mott}}}{\xi F_0} (1 - \frac{\pi}{16} \gamma^2 + \dots)\right) & \gamma \ll 1 (\text{tunneling}) \end{cases} \quad (36)$$

for AC fields $F(t) = F_0 \cos \Omega t$. The correlation length ξ characterizes the size of the doublon-hole pairs existing in the groundstate as a quantum fluctuation [136], and the Keldysh parameter which separates the tunneling dominant to multiphoton dominant creation is defined by $\gamma = \frac{\Omega}{F_0 \xi}$. Reaching and exceeding the Schwinger limit $F_{\text{Sch}} = \frac{\Delta_{\text{Mott}}}{\xi}$ is a challenging problem, and typically this is impossible since the electron avalanche occurs below the limit [121, 137] (also known in QED [138]). Recently, the Schwinger limit was reached and exceeded in correlated insulators, and the tunneling breakdown (Equation 36 lower) was experimentally verified [139, 140]. These outstanding result became possible by using a laser pulse that is short enough to suppress the heating and avalanche cascade effect.

VI. OUTLOOK

One of the most fascinating aspect of Floquet engineering is that it is becoming a common language for researchers with diverse backgrounds such as strongly correlated electron systems, artificial matter and nonequilibrium statistical mechanics. High energy physics and quantum field theory [130–133] is also a great source of ideas and motivations for condensed matter physicists and the interaction is expected to fertilize the field. As a closing, let us mention some challenges which may be interesting for future developments.

Tailored fields from metamaterial plasmonics: In order to make the Floquet engineered devices to fit inside our pockets, we need to replace the laser with a more efficient field generator, and the usage of metamaterials and near field optics will be an important step in this direction. Although it must be triggered by a pulse laser, metamaterials have demonstrated that an electric fields exceeding 1MV/cm [137] or a magnetic field of 1 Tesla [141], oscillating in the THz regime can be generated. Interestingly, the fields are “tailored” by the structure and is different from the traveling EM-field in the vacuum. It would be interesting to look for Floquet states that utilizes this freedom.

Phase transition in a nonequilibrium state: Strongly motivated by recent experiments on light-induced superconductivity [13, 115–117] several theoretical researches are done in driven correlated open systems [37, 41, 142]. The DC counterpart, *i.e.* phase transitions that occurs in non-linear devices [14–16, 34, 143], also show interesting properties [144], and provides challenges to theorists.

New device from new principle: It is interesting to look for functions of Floquet states that static systems cannot have. Devices that have an output signal with non-trivial frequencies due to the dynamics of the Floquet state have been proposed using correlated electrons [145, 146], two dimensional electron gas [147], and even single spins [148].

VII. DISCLOSURE STATEMENT

The authors are not aware of any affiliations, memberships, funding, or financial holdings that might be perceived as affecting the objectivity of this review.

VIII. ACKNOWLEDGMENTS

We gratefully acknowledge Naoto Tsuji, Takuya Kitagawa, Hideo Aoki, Shintaro Takayoshi, Masahiro Sato, Aditi Mitra, Hossein Dehghani, Takahiro Mikami, Eugene Demler, Liang Fu, André Eckardt and Achilleas Lazarides for useful discussions, and financial support from the Max Planck Society.

-
- [1] Nasu K. 2004. Photoinduced phase transitions. World Scientific
 - [2] Iwai S, Okamoto H. 2006. *J. Phys. Soc. Jpn.* 75:011007
 - [3] Koshihara S, Kuwata-Gonokami M. 2006. *J. Phys. Soc. Jpn.* 75:011001
 - [4] Yonemitsu K, Nasu K. 2008. *Physics Reports* 465:1–60
 - [5] Oka T, Aoki H. 2008. Nonequilibrium quantum breakdown in a strongly correlated electron system. In *Quantum and Semi-classical Percolation and Breakdown in Disordered Solids*. Springer Berlin Heidelberg, 1–35. (arXiv:0803.0422)

- [6] Kirilyuk A, Kimel AV, Rasing T. 2010. *Rev. Mod. Phys.* 82:2731–2784
- [7] Basov DN, Averitt RD, van der Marel D, Dressel M, Haule K. 2011. *Rev. Mod. Phys.* 83:471–541
- [8] Orenstein J. 2012. *Physics Today* 65:44–50
- [9] Aoki H, Tsuji N, Eckstein M, Kollar M, Oka T, Werner P. 2014. *Rev. Mod. Phys.* 86:779
- [10] Giannetti C, Capone M, Fausti D, Fabrizio M, Parmigiani F, Mihailovic D. 2016. *Advances in Physics* 65:58–238
- [11] Mankowsky R, Först M, Cavalleri A. 2016. *Rep. Prog. Phys.* 79:064503
- [12] Basov DN, Averitt RD, Hsieh D. 2017. *Nature Materials* 16:1077–1088
- [13] Cavalleri A. 2017. *Contemporary Physics* 59:31–46
- [14] Sawa A. 2008. *Materials Today* 11:28–36
- [15] Cario L, Vaju C, Corraze B, Guiot V, Janod E. 2010. *Advanced Materials* 22:5193–5197
- [16] Pan F, Gao S, Chen C, Song C, Zeng F. 2014. *Materials Science and Engineering: R: Reports* 83:1–59
- [17] Hasan MZ, Kane CL. 2010. *Rev. Mod. Phys.* 82:3045–3067
- [18] Qi XL, Zhang SC. 2011. *Rev. Mod. Phys.* 83:1057–1110
- [19] Castro Neto AH, Guinea F, Peres NMR, Novoselov KS, Geim AK. 2009. *Rev. Mod. Phys.* 81:109–162
- [20] Armitage NP, Mele EJ, Vishwanath A. 2018. *Rev. Mod. Phys.* 90:015001
- [21] Yan B, Felser C. 2017. *Annual Review of Condensed Matter Physics* 8:337–354
- [22] Imada M, Fujimori A, Tokura Y. 1998. *Rev. Mod. Phys.* 70:1039–1263
- [23] Shirley JH. 1965. *Phys. Rev.* 138:B979–B987
- [24] Dunlap DH, Kenkre VM. 1986. *Phys. Rev. B* 34:3625–3633
- [25] Sambe H. 1973. *Phys. Rev. A* 7:2203–2213
- [26] P. Hänggi. 1988. Quantum transport and dissipation, chap. 5. WILEY-VCH
- [27] Moskalets M, Büttiker M. 2002. *Phys. Rev. B* 66:205320
- [28] Grifoni M, Hänggi P. 1998. *Physics Reports* 304:229 – 354
- [29] Chu SI, Telnov DA. 2004. *Physics Reports* 390:1 – 131
- [30] Tsuji N, Oka T, Aoki H. 2008. *Phys. Rev. B* 78:235124
- [31] Oka T, Aoki H. 2008. *Phys. Rev. B* 78:241104
- [32] Tsuji N, Oka T, Aoki H. 2009. *Phys. Rev. Lett.* 103:047403
- [33] Heidrich-Meisner F, González I, Al-Hassanieh KA, Feiguin AE, Rozenberg MJ, Dagotto E. 2010. *Phys. Rev. B* 82:205110
- [34] Lee WR, Park K. 2014. *Phys. Rev. B* 89:205126
- [35] Mikami T, Kitamura S, Yasuda K, Tsuji N, Oka T, Aoki H. 2016. *Phys. Rev. B* 93:144307
- [36] Qin T, Hofstetter W. 2017. *Phys. Rev. B* 96:075134
- [37] Murakami Y, Tsuji N, Eckstein M, Werner P. 2017. *Phys. Rev. B* 96:045125
- [38] Murakami Y, Eckstein M, Werner P. 2017. *ArXiv e-prints* 1712.06460
- [39] Seetharam KI, Bardyn CE, Lindner NH, Rudner MS, Refael G. 2015. *Phys. Rev. X* 5:041050
- [40] Deghani H, Oka T, Mitra A. 2014. *Phys. Rev. B* 90:195429
- [41] Babadi M, Knap M, Martin I, Refael G, Demler E. 2017. *Phys. Rev. B* 96:014512
- [42] D’Alessio L, Rigol M. 2014. *Phys. Rev. X* 4:041048
- [43] Lazarides A, Das A, Moessner R. 2014. *Phys. Rev. E* 90:012110
- [44] D’Alessio L, Polkovnikov A. 2013. *Annals of Physics* 333:19 – 33
- [45] Kuwahara T, Mori T, Saito K. 2016. *Ann. Phys.* 367:96–124
- [46] Mori T, Kuwahara T, Saito K. 2016. *Phys. Rev. Lett.* 116:120401
- [47] Abanin D, Roeck WD, Ho WW, Huvneers F. 2017. *Communications in Mathematical Physics* 354:809–827
- [48] Ponte P, Chandran A, Papić Z, Abanin DA. 2015. *Annals of Physics* 353:196 – 204
- [49] Weinberg P, Bukov M, D’Alessio L, Polkovnikov A, Vajna S, Kolodrubetz M. 2017. *Physics Reports* 688:1 – 35. Adiabatic Perturbation Theory and Geometry of Periodically-Driven Systems
- [50] Goldman N, Dalibard J. 2014. *Phys. Rev. X* 4:031027
- [51] Eckardt A. 2017. *Rev. Mod. Phys.* 89:011004
- [52] Thouless DJ. 1983. *Phys. Rev. B* 27:6083–6087
- [53] Rice MJ, Mele EJ. 1982. *Phys. Rev. Lett.* 49:1455–1459
- [54] Kitagawa T, Berg E, Rudner M, Demler E. 2010. *Phys. Rev. B* 82:235114
- [55] Thouless DJ, Kohmoto M, Nightingale MP, den Nijs M. 1982. *Phys. Rev. Lett.* 49:405–408
- [56] Bukov M, D’Alessio L, Polkovnikov A. 2015. *Adv. Phys.* 64:139
- [57] Eckardt A, Anisimovas E. 2015. *New J. Phys.* 17:093039
- [58] Deutsch JM. 1991. *Phys. Rev. A* 43:2046–2049
- [59] Reimann P, Kastner M. 2012. *New J. Phys.* 14:043020
- [60] Berges J, Borsányi S, Wetterich C. 2004. *Phys. Rev. Lett.* 93:142002
- [61] Calabrese P, Cardy J. 2006. *Phys. Rev. Lett.* 96:136801
- [62] Moeckel M, Kehrein S. 2008. *Phys. Rev. Lett.* 100:175702
- [63] Mori T, Ikeda TN, Kaminishi E, Ueda M. 2017. *ArXiv e-prints* 1712.08790
- [64] Mitra A. 2018. *Annual Review of Condensed Matter Physics* 9:245–259
- [65] Casas F, Oteo JA, Ros J. 2001. *J. Phys. A: Math. Gen.* 34:3379
- [66] Mananga ES, Charpentier T. 2011. *J. Chem. Phys.* 135:044109
- [67] Pershan PS, van der Ziel JP, Malmstrom LD. 1966. *Phys. Rev.* 143:574–583
- [68] Mentink JH, Balzer K, Eckstein M. 2015. *Nat. Commun.* 6:6708

- [69] Bukov M, Kolodrubetz M, Polkovnikov A. 2016. *Phys. Rev. Lett.* 116:125301
- [70] Kitamura S, Oka T, Aoki H. 2017. *Phys. Rev. B* 96:014406
- [71] Claassen M, Jiang HC, Moritz B, Devereaux TP. 2017. *Nat. Commun.* 8
- [72] Oka T, Aoki H. 2009. *Phys. Rev. B* 79:081406
- [73] Haldane FDM. 1988. *Phys. Rev. Lett.* 61:2015–2018
- [74] Kitagawa T, Oka T, Brataas A, Fu L, Demler E. 2011. *Phys. Rev. B* 84:235108
- [75] Kitagawa T, Berg E, Rudner M, Demler E. 2010. *Phys. Rev. B* 82:235114
- [76] Lindner NH, Refael G, Galitski V. 2011. *Nat. Phys.* 7:490–495
- [77] Ishikawa T, Sagae Y, Naitoh Y, Kawakami Y, Itoh H, et al. 2014. *Nat. Commun.* 5:5528
- [78] Aharonov Y, Anandan J. 1987. *Phys. Rev. Lett.* 58:1593–1596
- [79] Berry MV. 1984. *Proceedings of the Royal Society A: Mathematical, Physical and Engineering Sciences* 392:45–57
- [80] Wang YH, Steinberg H, Jarillo-Herrero P, Gedik N. 2013. *Science* 342:453–457
- [81] Jotzu G, Messer M, Desbuquois R, Lebrat M, Uehlinger T, et al. 2014. *Nature* 515:237
- [82] Rechtsman MC, Zeuner JM, Plotnik Y, Lumer Y, Podolsky D, et al. 2013. *Nature* 496:196–200
- [83] Torres M, Kunold A. 2005. *Phys. Rev. B* 71:115313
- [84] Dehghani H, Oka T, Mitra A. 2015. *Phys. Rev. B* 91:155422
- [85] Oka T, Aoki H. 2010. *Journal of Physics: Conference Series* 334:5
- [86] Ikebe Y, Morimoto T, Masutomi R, Okamoto T, Aoki H, Shimano R. 2010. *Phys. Rev. Lett.* 104:256802
- [87] Gu Z, Fertig HA, Arovas DP, Auerbach A. 2011. *Phys. Rev. Lett.* 107:216601
- [88] Žutić I, Fabian J, Das Sarma S. 2004. *Rev. Mod. Phys.* 76:323–410
- [89] Kimel AV, Kirilyuk A, Usachev PA, Pisarev RV, Balbashov AM, Rasing T. 2005. *Nature* 435:655–657
- [90] Stanciu CD, Hansteen F, Kimel AV, Kirilyuk A, Tsukamoto A, et al. 2007. *Phys. Rev. Lett.* 99:047601
- [91] Tokura Y, Seki S, Nagaosa N. 2014. *Rep. Prog. Phys.* 77:076501
- [92] Tanabe Y, Moriya T, Sugano S. 1965. *Phys. Rev. Lett.* 15:1023–1025
- [93] Katsura H, Nagaosa N, Balatsky AV. 2005. *Phys. Rev. Lett.* 95:057205
- [94] Sato M, Sasaki Y, Oka T. 2014. *ArXiv e-prints* 1404.2010
- [95] Sato M, Takayoshi S, Oka T. 2016. *Phys. Rev. Lett.* 117:147202
- [96] Takayoshi S, Aoki H, Oka T. 2014. *Phys. Rev. B* 90:085150
- [97] Takayoshi S, Sato M, Oka T. 2014. *Phys. Rev. B* 90:214413
- [98] Kaminski A, Nazarov YV, Glazman LI. 2000. *Phys. Rev. B* 62:8154–8170
- [99] Goldin Y, Avishai Y. 2000. *Phys. Rev. B* 61:16750–16772
- [100] Kugel KI, Khomskii DI. 1982. *Soviet Physics Uspekhi* 25:231–256
- [101] Eckstein M, Mentink JH, Werner P. 2017. *ArXiv e-prints* 1703.03269
- [102] Chaloupka Jcv, Jackeli G, Khaliullin G. 2010. *Phys. Rev. Lett.* 105:027204
- [103] Bhattacharjee S, Lee SS, Kim YB. 2012. *New Journal of Physics* 14:073015
- [104] Kitaev A. 2006. *Annals of Physics* 321:2 – 111. January Special Issue
- [105] Bauer B, Cincio L, Keller BP, Dolfi M, Vidal G, et al. 2014. *Nat. Commun.* 5:5137
- [106] Shimizu Y, Miyagawa K, Kanoda K, Maesato M, Saito G. 2003. *Phys. Rev. Lett.* 91:107001
- [107] Koshihara S, Tokura Y, Mitani T, Saito G, Koda T. 1990. *Phys. Rev. B* 42:6853–6856
- [108] Koshihara S, Tokura Y, Takeda K, Koda T. 1992. *Phys. Rev. Lett.* 68:1148–1151
- [109] Cavalleri A, Tóth C, Siders CW, Squier JA, Ráksi F, et al. 2001. *Phys. Rev. Lett.* 87:237401
- [110] Yu G, Lee CH, Heeger AJ, Herron N, McCarron EM. 1991. *Phys. Rev. Lett.* 67:2581–2584
- [111] Iwai S, Ono M, Maeda A, Matsuzaki H, Kishida H, et al. 2003. *Phys. Rev. Lett.* 91:057401
- [112] Perfetti L, Loukakos PA, Lisowski M, Bovensiepen U, Eisaki H, Wolf M. 2007. *Phys. Rev. Lett.* 99:197001
- [113] Wall S, Brida D, Clark SR, Ehrke HP, Jaksch D, et al. 2010. *Nature Physics* 7:114–118
- [114] Strohmaier N, Greif D, Jördens R, Tarruell L, Moritz H, et al. 2010. *Phys. Rev. Lett.* 104:080401
- [115] Fausti D, Tobey RI, Dean N, Kaiser S, Dienst A, et al. 2011. *Science* 331:189–191
- [116] Hu W, Kaiser S, Nicoletti D, Hunt CR, Gierz I, et al. 2014. *Nature Materials* 13:705–711
- [117] Kaiser S, Hunt CR, Nicoletti D, Hu W, Gierz I, et al. 2014. *Phys. Rev. B* 89:184516
- [118] Tokura Y, Okamoto H, Koda T, Mitani T, Saito G. 1988. *Phys. Rev. B* 38:2215–2218
- [119] Asamitsu A, Tomioka Y, Kuwahara H, Tokura Y. 1997. *Nature* 388:50–52
- [120] Taguchi Y, Matsumoto T, Tokura Y. 2000. *Phys. Rev. B* 62:7015–7018
- [121] Guiot V, Cario L, Janod E, Corraze B, Phuoc VT, et al. 2013. *Nat. Commun.* 4:1722
- [122] Hirori H, Shinokita K, Shirai M, Tani S, Kadoya Y, Tanaka K. 2011. *Nat. Commun.* 2:594
- [123] Oka T, Arita R, Aoki H. 2003. *Phys. Rev. Lett.* 91:066406
- [124] Oka T, Aoki H. 2005. *Phys. Rev. Lett.* 95:137601
- [125] Takahashi A, Itoh H, Aihara M. 2008. *Phys. Rev. B* 77:205105
- [126] Oka T, Aoki H. 2010. *Phys. Rev. B* 81:033103
- [127] Tsuji N, Oka T, Werner P, Aoki H. 2011. *Phys. Rev. Lett.* 106:236401
- [128] Oka T. 2012. *Phys. Rev. B* 86:075148
- [129] Bukov M, Kolodrubetz M, Polkovnikov A. 2016. *Phys. Rev. Lett.* 116:125301
- [130] Heisenberg W, Euler H. 1936. *Zeitschrift für Physik* 98:714–732. (translated to English in arXiv:0605038)
- [131] Schwinger J. 1951. *Phys. Rev.* 82:664–679
- [132] Dunne GV. 2009. *The European Physical Journal D* 55:327–340

- [133] Gelis F, Tanji N. 2016. *Progress in Particle and Nuclear Physics* 87:1–49
- [134] Resta R. 1994. *Rev. Mod. Phys.* 66:899–915
- [135] King-Smith RD, Vanderbilt D. 1993. *Phys. Rev. B* 47:1651–1654
- [136] Stafford CA, Millis AJ. 1993. *Phys. Rev. B* 48:1409–1425
- [137] Liu M, Hwang HY, Tao H, Strikwerda AC, Fan K, et al. 2012. *Nature* 487:345–348
- [138] Fedotov AM, Narozhny NB, Mourou G, Korn G. 2010. *Phys. Rev. Lett.* 105:080402
- [139] Mayer B, Schmidt C, Grupp A, Bühler J, Oelmann J, et al. 2015. *Phys. Rev. B* 91:235113
- [140] Yamakawa H, Miyamoto T, Morimoto T, Terashige T, Yada H, et al. 2017. *Nature Materials* 16:1100–1105
- [141] Mukai Y, Hirori H, Yamamoto T, Kageyama H, Tanaka K. 2016. *New Journal of Physics* 18:013045
- [142] Knap M, Babadi M, Refael G, Martin I, Demler E. 2016. *Phys. Rev. B* 94:214504
- [143] Rozenberg MJ, Inoue IH, Sánchez MJ. 2004. *Phys. Rev. Lett.* 92:178302
- [144] Sow C, Yonezawa S, Kitamura S, Oka T, Kuroki K, et al. 2017. *Science* 358:1084–1087
- [145] Silva REF, Blinov IV, Rubtsov AN, Smirnova O, Ivanov M. 2018. *Nature Photonics*
- [146] Murakami Y, Eckstein M, Werner P. 2017. *ArXiv e-prints* 1712.06460
- [147] Oka T, Bucciantini L. 2016. *Phys. Rev. B* 94:155133
- [148] Martin I, Refael G, Halperin B. 2017. *Phys. Rev. X* 7:041008